Annals of Phytomedicine 14(1): 559-568, 2025

DOI: http://dx.doi.org/10.54085/ap.2025.14.1.53

Annals of Phytomedicine: An International Journal
http://www.ukaazpublications.com/publications/index.php

Print ISSN : 2278-9839 Online ISSN : 2393-9885

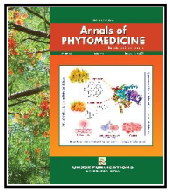

Original Article : Open Access

Novel thiadiazole derivatives targeting acetylcholinesterase in Alzheimer's disease: Synthesis and biological evaluation

E. Joel Mart and C. Ronald Darwin◆

Department of Pharmacology, School of Pharmaceutical Sciences, Vels Institute of Science, Technology and Advanced Studies (VISTAS), Pallavaram-600117, Chennai, Tamil Nadu, India

Article Info

Article history
Received 2 April 2025
Revised 15 May 2025
Accepted 16 May 2025
Published Online 30 June 2025

Keywords
1,3,4-Thiadiazole derivatives
Cell viability
Acetylcholinesterase inhibition
Neuroprotection
Alzheimer's disease
SH-SY5Y cells

Abstract

Acetylcholine levels are decreased frequently linked to Alzheimer's disease (AD), a progressive neurodegenerative illness marked by memory loss and cognitive impairment, as a result of increased acetylcholinesterase (AChE) activity. Several new thiadiazole compounds were synthesized for this investigation, and their potential as neuroprotective and AChE inhibitors was evaluated. The synthetic route involved the initial formation of 2-(5-amino-1,3,4-thiadiazol-2-yl)-5-bromophenol using thiosemicarbazide and 4-bromo salicylic acid, followed by Schiff base condensation with various substituted aromatic and heteroaromatic aldehydes. All compounds were structurally characterized by IR, ^{1}H and C13NMR, and mass spectroscopy and confirmed for purity. Molecular docking studies against acetylcholinesterase (PDB ID: 4EY6) revealed strong binding affinities, particularly for compound T3 [(E)-2-(5-((4-aminobenzylidene)amino)-1,3,4-thiadiazol-2-yl)-5-bromophenol], which exhibited notable hydrogen bonding and hydrophobic interactions at the AChE active site. *In vitro* MTT assays on neuronal cells demonstrated that T3 significantly enhanced cell viability, indicating potent neuroprotective activity with low cytotoxicity, even outperforming the standard drug used as a reference.

The novelty of this work lies in the strategic integration of pharmacologically active moieties within a single molecular scaffold, offering dual benefits of AChE inhibition and neuroprotection. Additionally, efforts to minimize toxicity through molecular design, and early-stage biological screening underscore the compound's promise as a safe therapeutic candidate for AD. These results provide support for the potential of derivatives based on thiadiazole in the creation of strong medications that target neuro degenerative illnesses.

1. Introduction

Alzheimer's disease (AD) is a progressive neurodegenerative disorder characterized by cognitive decline, memory impairment, and changes in behavior. Acetylcholine (ACh) deficit in the brain is a major pathophysiological feature of AD. This is mainly caused by excessive activity of the enzyme acetylcholinesterase (AChE), which hydrolyzes ACh. One proven treatment method to improve cholinergic neurotransmission and reduce AD symptoms is to inhibit AChE (Ahmad Mohammadi Faran *et al.,* 2024). Current AChE inhibitors, such as donepezil, rivastigmine, and galantamine, offer symptomatic relief but are often associated with adverse effects and limited efficacy. This underscores the need for novel AChE inhibitors with improved safety profiles and additional neuroprotective properties (Makhaeva *et al.,* 2023). Heterocyclic compounds (Afroz patan *et al.,* 2023), particularly 1,3,4-thiadiazole derivatives, have garnered attention due to their diverse pharmacological activities, including antimicrobial (Anthwal *et al.,* 2022), anti-inflammatory (Halit Muðlu *et al.,* 2022), antioxidant (Gowda *et al.,* 2022), anticancer (Chandra Sekhar *et al.,* 2019, Shaikh *et al.,* 2024), antitumor (Altintop *et al.,* 2018) and neuroprotective effects (Hatami *et al.,* 2023). Incorporating electron-rich nitrogen and sulfur atoms in the thiadiazole ring enhances binding affinity to enzyme targets through hydrogen bonding and hydrophobic interactions (Zahid Ali *et al.,* 2023). Moreover, the functionalization of thiadiazole with phenolic and Schiff base moieties has been reported to improve biological activity and metabolic stability. Recent studies have demonstrated the potential of thiadiazole-based compounds as AChE inhibitors (Pham *et al.,* 2022). For instance, novel 2,5-disubstituted-1,3,4-thiadiazole derivatives exhibited dual inhibition activity against cholinesterases and monoamine oxidases, enzymes implicated in AD pathology (Makhaeva *et al.,* 2020). Additionally, indazole-based thiadiazole-bearing thiazolidinone hybrids showed significant AChE inhibitory activity (Sindhu *et al.,* 2024), with some compounds displaying IC_{50} values comparable to or better than donepezil (Elkina *et al.,* 2022).

In this context, the present study focuses on the design, synthesis, and evaluation of (*E*)-2-(5-((arylidene)amino)-1,3,4-thiadiazol-2-yl)-5-bromophenol derivatives as potential AChE inhibitors with neuroprotective properties. The synthetic approach involves the initial formation of (*E*)-2-(5-amino-1,3,4-thiadiazol-2-yl)-5-

Corresponding author: Dr. C. Ronal Darwin
Professor, Department of Pharmacology, School of Pharmaceutical Sciences, Vels Institute of Science, Technology and Advanced Studies (VISTAS) Pallavaram-600117, Chennai, Tamil Nadu, India
E-mail: ronaldpharma@gmail.com
Tel.: +91-9444428759

bromophenol, followed by condensation with various substituted aromatic and heteroaromatic aldehydes to yield Schiff base derivatives (Kumar *et al.,* 2022). These compounds are characterized using IR, NMR, and mass spectrometry, and their biological activities are assessed through molecular docking studies (Malarkodi Velraj *et al.,* 2024) against AChE (PDB ID: 4EY6) and *in vitro* MTT assays to evaluate cytotoxicity and neuroprotective potential. This integrative approach aims to identify novel thiadiazole-based scaffolds with enhanced efficacy and safety profiles, contributing to developing effective therapeutic agents for Alzheimer's disease (Patel *et al.,* 2020).

2. Methods and Materials

Compounds T1, T2, T3, T4 and T5 of five new thiadiazole derivatives (Table 1) were designed and synthesized. Commercial chemicals and solvents were purchased from Merck, India, for use in experimental operations.

Table 1: Novel thiadiazole derivatives

Compounds	Structures
T 1	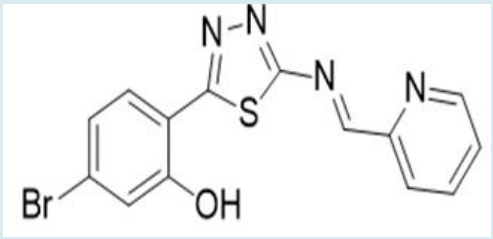
T 2	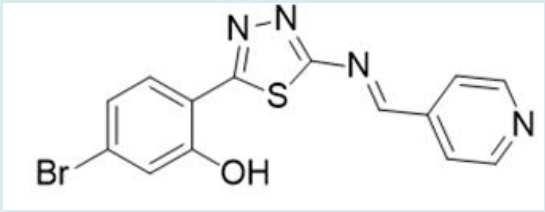
T 3	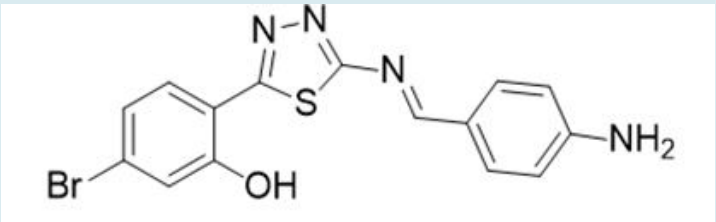
T 4	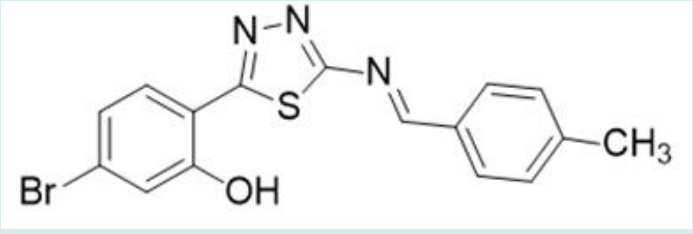
T 5	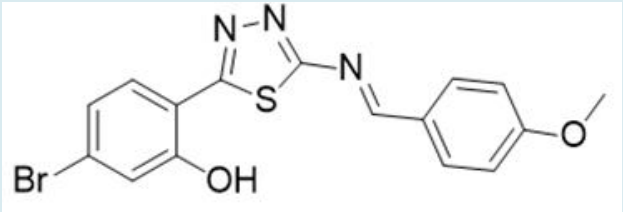

2.1 General procedure for the synthesis of thiadiazole derivatives

2.1.1 Step 1 (Compound A)

About 50 mmol of 4-bromo-salicylic acid and 50 mmol of thiosemicarbazide with 13.0 ml of phosphoryl chloride ($POCl_2$), were heated for 35-45 min in a fuming cupboard at 65 to 75°C in an RB flask. After bringing the contents' temperature down to 27°C (1 h) in an ice bath, 100 ml of distilled water was added, first dropwise and then gradually in 5-7 ml portions when the fuming stopped. After that, a reflux condenser was fixed, and the contents were heated for roughly 22 to 24 h. Using n-hexane: ethyl acetate (5:5) as a mobile phase, TLC was used to track the reaction's conclusion. 50% NaOH was added while swirling constantly to cool and basify the liquid. After the product was air-dried, the filtered solids were cleaned with distilled water. Ethanol was utilized for recrystallization (Chen *et al.,* 2022).

The phosphoryl chloride ($POCl_2$) acts as a dehydrating agent, cyclizing thiosemicarbazide and 4-bromo-salicylic acid to promote the formation of a thiazole ring. This step involves the formation of an intermediate through cyclization. (E)-2-(5-amino-1,3,4-thiadiazol-2-yl)-5-bromophenol intermediate compounds were formed. The intermediate compound was stabilized upon cooling. The gradual addition of distilled water helps hydrolyze any excess $POCl_2$ and dissolve it, preventing further reaction. The final product was formed during reflux as a result of further cyclization and dehydration of the intermediate. The temperature and prolonged heating ensure the reaction completion. Thin layer chromatography (TLC) is used to monitor the reaction progress. n-Hexane and ethyl acetate (5:5) serve as the mobile phase to separate the components based on their polarity. The mixture was basified with 50% NaOH to neutralize the acidic components and precipitate the product. The continuous stirring ensures uniform distribution (Ahmed *et al.,* 2020).

2.1.2 Step 2

The reaction mixture was prepared by adding compound A (0.01 mol) to 10-12 ml of 100% ethyl alcohol in a 25 ml round-bottom flask, with NaOH pellets used as the catalyst. This mixture was then used to reflux the corresponding aromatic and heteroaromatic aldehydes (0.01 mmol). The synthesis of compounds T1, T2, T3, T4 and T5 by using heteroaromatic aldehydes were pyridin-2-carbaldehyde, pyridin-4-carbaldehyde, para amino benzaldehyde, para methyl benzaldehyde and para methoxy benzaldehyde respectively. TLC used a MP of ethyl acetate: n-hexane (5:5) to track the reaction development. The contents were poured into a petri plate after the reaction was completed. The solvent was allowed to evaporate by air. To remove any excess base, the product was washed with diluted HCl for neutralization (Li *et al.,* 2021).

Compound A was dissolved in ethyl alcohol, and NaOH pellets were added as a base catalyst. The NaOH will deprotonate compound A, making it more reactive. The mixture was refluxed with the aromatic and hetero aromatic aldehydes. During reflux, the reaction mixture was heated to its boiling point, causing the aldehydes to react with the intermediate formed in step 1. This typically involves nucleophilic addition or condensation reactions, depending on the nature of Compound A. TLC was utilized to monitor the progress of the reaction. A mobile phase composed of ethyl acetate and n-hexane in a 5:5 ratio facilitated the separation of compounds based on their polarity. Identification of the completion of the reaction by observing the appearance/disappearance of spots on the TLC plate. After confirming the reaction completion, the reaction mixture is poured into a petri dish. The solvent (ethyl alcohol) was allowed to evaporate by air, leaving behind the solid product. The solid product was washed with diluted HCl to neutralize any excess base (NaOH) present in the mixture. This step ensures that the product is free from any residual alkaline impurities (Kumar *et al.,* 2023).

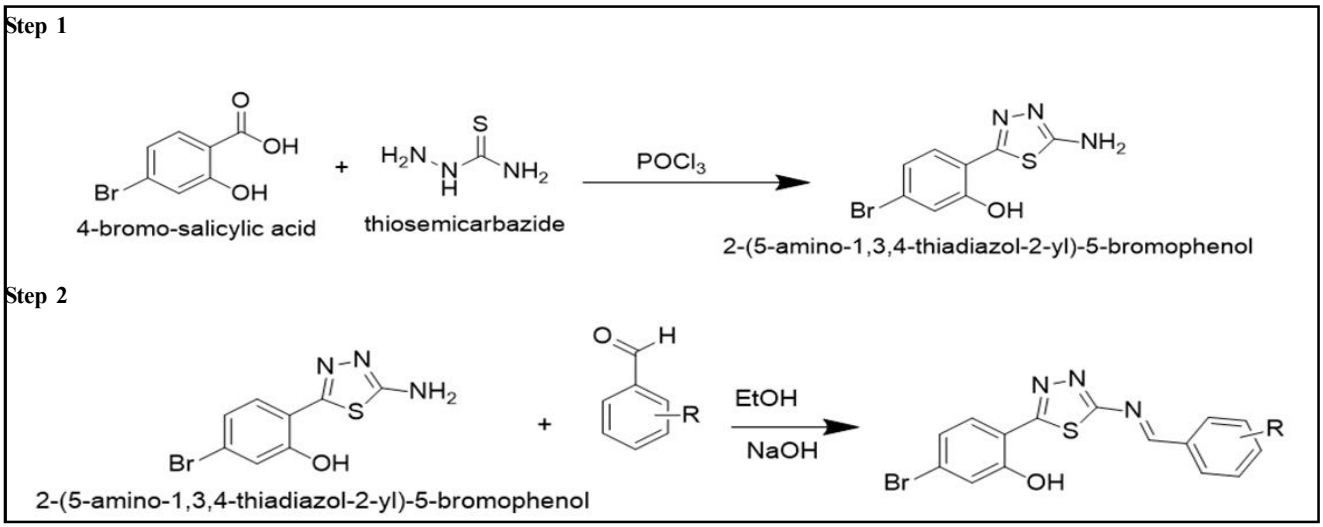

Figure 1: Schematic diagram for the synthesis of thiadiazole derivatives.

2.2 *In silico* molecular docking study

In contemporary drug design, docking techniques are commonly employed to examine the interaction between a ligand and its receptor, as well as to determine how the lead compound binds and aligns with its target protein receptor. Associating target components is a common use case. The research was conducted in a virtual environment using bioinformatics technologies. Additionally, offline resources such as the PubChem database, Marvin Sketch, and Protein Data Bank (PDB), were utilized. Molecular docking experiments were performed using PyRx 0.9.

2.2.1 Protein preparation

With the PDB (PDB ID: 4EY6) offline application, we were able to obtain a resolution of 1.90Å for the acetylcholinesterase (PDB: 4EY6). After eliminating the protein crystal water, the missing hydrogens were added, and protonation, ionization, and energy minimization were performed to purify the protein (4EY6). The SPDBV force field was employed for energy minimization. The integrity of the produced protein was confirmed using the Ramachandran plot.

2.2.2 Ligand preparation

The Marvin Sketch tool can generate both two and three dimensional molecular models. Once the molecule is created, it is processed in 3D using Marvin Sketch and then saved as a PDB file.

2.2.3 Active site identification

The PDB ID was selected and uploaded using the protein ligand interaction profile (PLIP) offline tool. Interactions between the protein and ligand, intra-chain interactions, and interactions between chains were selected. Thresholds were adjusted to detect interactions such as hydrogen bonds, salt bridges, and hydrophobic contacts. The file was submitted, and the analysis was completed. The PLIP tool automatically detected and visualized the interactions between the protein and ligand, providing atom-level characterization. The interaction report was examined, and the active amino acids binding with the ligands were identified. The PLIP online tool is used to identify the active amino acid present in the protein. This allowed us to identify the protein's active amino acid.

2.2.4 Procedure for molecular docking

In the market coordinates in PDB format, the PyRx virtual screening tool demonstrated a greater docking accuracy than the other docking product stages (Glide: 82%, MVD : 87%, FlexX: 58%, and Surflex: 75%). The receptor file was cleared of non-polar hydrogen atoms, and the matching carbon atoms were given their partial charges. PyRx software's molecular docking engine was used to carry out molecular docking. A spherical area that includes every protein atom within 15.0 A of the bound crystallographic ligand atom was identified as the binding site. All computations were performed using the default parameters. A grid resolution was used for docking.

2.3 *In vitro* evaluation of neuroprotective activity of synthesized compounds by MTT assay method

The MTT assay is a color-based method utilized to evaluate cellular metabolic activity. NAD(P)H-dependent cellular oxido reductase enzymes can, in some cases, indicate the number of viable cells in a sample. The tetrazolium dye (E)-3-(4,5-dimethylthiazol-2-yl)-2,5-diphenyltetrazolium bromide (MTT) can be chemically reduced by these enzymes to form an insoluble purple formazan. The number of viable cells is closely correlated with the intensity of the purple color, which can be used to calculate the percentage of cell viability (Patel *et al.,* 2021).

2.3.1 Cell culture

A batch of human SH-SY5Y neuroblastoma cells from Sigma Aldrich were cultivated at 37°C in a humidified environment with 5.0% CO_2 in dulbecco's modified eagle medium (DMEM) supplemented with 10% fetal bovine serum (FBS). After the cells achieved 80% confidence, investigations were carried out.

2.3.2 Cell viability determination

The cell viability was confirmed by, we employed a conventional MTT reduction experiment. The experiment was conducted in three different runs. Cells were seeded in 96-well plates using 10% FBS and 100 µl supplement at an average density of 2.0×10^4 cells/ healthy. The cells were pretreated for 2 h with five different dosages of test compounds (50, 100, 200, and 400 µg/ml, dispersed in DMEM with 10% FBS) following a 24 h stabilization phase. The therapy was mixed with 10 µM Aβ25-35 after 2 h and left to incubate at 37.0°C in 5.0% CO_2 for a further 24 h. In statistical experiments, the condition was using 10% FBS with DMEM solvent. Following the treatment conclusion, each well containing an MTT (100 µl), and the plates were incubated for 4 h while the culture media was discarded.

To dissolve the dark blue crystals, 100 µl of DMSO was applied to each well after the MTT solution was removed. A thermal plate scanner was used to scan the plates at 540 nm after they had been shaking for a short time. Percentages showed the analytical results in comparison to the control group (Zhang *et al.,* 2022).

2.3.3 Working and stock solutions preparation

About 30 ml of cell culture medium and 70 ml of alcohol were measured and transferred into a sterile container. It helps to prevent potential damage to the proteins or other sensitive components of the medium. Vacuum filtration was utilized for the filtration process. The mixture was poured into the filtration unit and filtered under sterile conditions. The filtered solution was transferred into a sterile, capped storage container. The container was placed in a refrigerator set at 4°C for storage. The stock solution's final concentration of 4.0×10^3 g/ml was diluted in the cell medium, to determine the volume of stock solution needed based on its concentration.

2.3.4 Working solution and stock solution for Aβ25-35

The concentration of Aβ25-35 in the sterile distilled water was 1.0 ml. The 100 µM working solution was used in a cell medium that also included 10% FBS for the treatments, resulting in an endpoint concentration of 10 µM in very well. The Cell inhibition percentage was determined using the following formula:

$$\% \text{ Cell inhibition} = \frac{\text{Control OD} - \text{Sample OD}}{\text{Control OD}} \times 100$$

$$\% \text{ Cell viability} = 100 - \text{Cell inhibition}$$

By analyzing the dose-response curves for each cell line, we were able to determine the smallest concentration of the test samples that would prevent 50% of the cell growth.

3. Results

3.1 Spectral analysis of synthesized compound (T1-T5)

(E)-5-bromo-2-(5-((pyridine-2-ylmethylene) amino)-1,3,4-thiadiazol-2-yl)phenol (T1)

Compound T1 was synthesized according to the general procedure. Molecular formula: Chemical Formula: $C_{14}H_9BrN_4OS$, Yield 88%. Rf value: 0.92. FT-IR (ν, cm^{-1}): A broad peak around 3366–3284 cm^{-1} indicated the presence of O–H and N–H stretching vibrations, suggesting phenolic and amine functionalities. The band at 3064 cm^{-1} corresponds to aromatic C–H stretching, confirming aromaticity. The sharp peak at 1651 cm^{-1} indicated C=N stretching, characteristic

of a Schiff base linkage formed through condensation between an amine and aldehyde. Additional bands at 1521, 1367, and 1311 cm^{-1} suggest aromatic C=C stretching and C–N/C–O functionalities, confirming the heterocyclic thiadiazole ring and phenol substitution. Peaks at 1085 and 812 cm^{-1} correspond to C–N stretching, aromatic C–H out-of-plane bending, and aromatic C–H stretching the band at 723 cm^{-1} provides strong evidence for the successful synthesis of the brominated thiadiazole derivative. m/z: calculated for m/z: 359.97 (100.0%), 361.97 (98.9%), 360.97 (17.6%), 362.97 (16.4%), 361.96 (4.5%), 363.96 (4.4%), 363.97 (1.6%), 362.96 (1.5%). ^{1}H nuclear magnetic resonance spectra in DMSO at 500 MHz show the following patterns: 9.82 (s, 1H), 8.67 (s, 1H), 8.51 (s, 1H), 7.87 (s, 1H), 7.80 (s, 1H), 7.51 (s, 1H), 7.30 (s, 1H), 7.14 (d, J = 17.9 Hz, 2H), The ^{13}C NMR spectrum at 126 MHz in DMSO shows peaks at: γ 171.34, 170.31, 155.68, 134.65, 134.34, 129.99, 129.36, 129.30, 128.79, 128.02, 127.88, 127.26, 127.02, 126.63, 124.45, 123.71, 40.54. Elemental Analysis: C, 46.55; H, 2.51; Br, 22.12; N, 15.51; O, 4.43; S, 8.88.

(E)-5-bromo-2-(5-((pyridine-4-ylmethylene)amino)-1,3,4-thiadiazol-2-yl)phenol (T2)

Compound T2 was synthesized according to the general procedure. Molecular formula $C_{14}H_9BrN_4O_S$. Yield 76%. MP: 176-179ÚC. Rf value: 0.89. FT-IR (ν, cm^{-1}): A distinct peak around 723 cm^{-1} is attributed to C–Br stretching, confirming the retention of the bromine atom at the aromatic ring position, a vital structural feature of the brominated phenol moiety. The broad absorption near 3349-3205 cm^{-1} indicated O–H and N–H stretching vibrations, corresponding to the phenolic and amine functionalities. The strong band at 1652 cm^{-1} supports the presence of the C=N stretching vibration from the imine (Schiff base) linkage. Additionally, bands around 1590 cm^{-1} and 1522 cm^{-1} correspond to aromatic C=C stretching, while peaks in the region of 1150-850 cm^{-1} may be attributed to C–N stretching and other fingerprint region vibrations. m/z: calculated for T2 for 359.97 observed m/z: 359.97 (100.0%), 361.97 (98.9%), 360.97 (17.6%), 362.97 (16.4%), 361.96 (4.5%), 363.96 (4.4%), 363.97 (1.6%), 362.96 (1.5%). The ^{1}H NMR spectrum of the compound was recorded at 500 MHz in DMSO as follows: γ 9.82 (s, 1H), 8.67 (s, 1H), 8.51 (s, 1H), 7.87 (s, 1H), 7.80 (s, 1H), 7.51 (s, 1H), 7.30 (s, 1H), 7.14 (d, J = 17.9 Hz, 2H), The chemical shifts observed in the ^{13}C NMR spectrum at 126 MHz in DMSO ä 171.34, 170.31, 155.68, 134.65, 134.34, 129.99, 129.36, 129.30, 128.79, 128.02, 127.88, 127.26, 127.02, 126.63, 40.54. Elemental Analysis: C, 46.55; H, 2.51; Br, 22.12; N, 15.51; O, 4.43; S, 8.88

(E)-2-(5-((4-aminobenzylidene)amino)-1,3,4-thiadiazol-2-yl)-5-bromophenol (T3)

Compound T3 was synthesized according to the general procedure. Molecular formula $C_{15}H_{11}BrN_4O_S$. Yield 75%. MP: 176-179ÚC. Rf value: 0.83. FT-IR (ν, cm^{-1}): The peak at 722 cm^{-1} corresponds to C–Br stretching, indicating the presence of the bromine-substituted aromatic ring, which is essential for biological activity. Strong broadband around 3368–3066 cm^{-1} corresponds to O–H and N–H stretching, indicative of phenolic and amino functionalities. The absorption band near 1652 cm^{-1} characteristic of C=N stretching, confirming the formation of the Schiff base (imine) linkage. The aromatic C=C stretching is observed in the region of 1590 – 1520 cm^{-1}, while additional peaks between 1150 and 850 cm^{-1} may be attributed to C–N stretching and other skeletal vibrations. m/z: calculated for T3 for 375.24 observed 373.98 m/z: 375.98 (100.0%), 373.98 (98.0%), 374.99 (16.1%), 376.99 (15.7%), 377.98 (4.7%), 376.98 (3.0%), 374.98 (2.2%), 375.99 (1.6%), 377.99 (1.5%). The compound ^{1}H NMR spectra were recorded in DMSO at 500 MHz as follows: ä 9.89 (s, 1H), 9.75 (m, 2H), 8.52 (s, 1H), 7.31 (s, 1H), 7.14 (d, J = 18.4 Hz, 2H), 6.68-6.53 (m, 2H), 6.53-6.44 (m, 2H). ^{13}C NMR spectra recorded in DMSO at 126 MHz show chemical shifts of ä 168.50, 156.63, 148.92, 148.39, 125.64, 121.60, 109.19, 106.92, 106.34, 102.06, 40.53. Elemental Analysis: C, 48.01; H, 2.95; Br, 21.29; N, 14.93; O, 4.26; S, 8.55.

(E)-5-bromo-2-(5-((4-methylbenzylidene)amino)-1,3,4-thiadiazol-2-yl)phenol (T4)

Compound T4 was synthesized according to the general procedure. Molecular formula $C_{16}H_{12}BrN_3OS$. Yield 73 %. MP: 176-179ÚC. Rf value: 0.81. FT-IR (ν, cm^{-1}): A prominent peak at 748 cm^{-1} indicates C–Br stretching, confirming the presence of a brominated aromatic ring. The broad bands between 3370-3060 cm^{-1} are characteristic of O–H and N–H stretching vibrations, associated with phenolic and amine groups. The C=N stretching vibration of the imine (Schiff base) is observed at 1593 cm^{-1}, affirming successful condensation with aromatic aldehydes. Peaks in the region of 1653-1517 cm^{-1} correspond to aromatic C=C and C=N stretching, while the bands near 1152-813 cm^{-1} are due to C–N stretching and aromatic C–H bending. m/z: calculated for T4 for 374.25 observed m/z: 372.99 (100.0 %), 374.99 (97.8 %), 373.99 (19.4 %), 375.99 (18.6 %), 374.98 (4.5 %), 376.98 (4.4 %), 376.99 (2.0 %), 375.00 (1.4 %), 375.98 (1.1 %). The ^{1}H NMR spectrum of the compound was recorded at 500 MHz in DMSO as follows: ^{1}H NMR (500 MHz, DMSO) ™ 9.82 (s, 1H), 8.63 (s, 1H), 7.31 (s, 1H), 7.14 (d, J = 18.4 Hz, 2H), 7.11-7.00 (m, 2H), 6.85-6.71 (m, 2H), 2.38-2.34 (m, 3H).

The chemical shifts observed in the ^{13}C NMR spectrum at 126 MHz in DMSO are ä 168.50, 156.63, 148.92, 148.39, 125.64, 121.60, 109.19, 106.92, 106.34, 102.06, 40.53, 20.90, 19.18, 17.47. Elemental Analysis: C, 51.35; H, 3.23; Br, 21.35; N, 11.23; O, 4.27; S, 8.57

(E)-5-bromo-2-(5-((4-methoxy benzylidene)amino)-1,3,4-thiadiazol-2-yl)phenol- (T5)

Compound T5 was synthesized according to the general procedure. Molecular formula $C_{16}H_{12}BrN_3O_2S$. Yield 79%. MP: 176-179ÚC. Rf value: 0.89. FT-IR (ν, cm^{-1}): The broad peaks around 3367-3050 cm^{-1} indicate O–H and N–H stretching vibrations, suggestive of hydroxyl or amine functionalities. The C=N stretching of the imine group is observed near 1591 cm^{-1}, characteristic of Schiff base linkages. Additional peaks at 1654 cm^{-1} and 1521 cm^{-1} are indicative of C=C stretching in aromatic rings, supporting the presence of a conjugated system. The absorption at 1147 cm^{-1} may be attributed to C–N or C–O stretching, while the band at 852 cm^{-1} corresponds to C-Br stretching, confirming the incorporation of a brominated aromatic ring. m/z: calculated for T5 for 388.98 observed m/z: 390.98 (100.0%), 388.98 (98.0%), 391.98 (19.1%), 389.99 (17.2%), 392.98 (4.7%), 390.99 (2.0%), 389.98 (1.9%), 392.99 (1.8%), The 1H NMR spectrum of the compound was recorded at 500 MHz in DMSO as follows: ^{1}H NMR (500 MHz, DMSO) ä 9.84 (s, 1H), 8.63 (s, 1H), 7.31 (s, 1H), 7.14 (d, J = 18.4 Hz, 2H), 7.11-7.00 (m, 2H), 6.85-6.71 (m, 2H), 2.38-2.34 (m, 3H). The chemical shifts observed in the ^{13}C NMR spectrum at 126 MHz in DMSO are 170.30, 155.81, 154.37, 134.50, 130.00, 129.31, 128.03, 127.26, 127.03, 124.45, 119.01, 108.40, 24.85. Elemental Analysis: C, 49.24; H, 3.10; Br, 20.47; N, 10.77; O, 8.20; S, 8.22

3.2 Docking study results

Docking using PyRx 0.9 was performed on the five synthesized molecules. Despite having various docking scores, the findings demonstrated that all derivatives have a nearly identical binding mechanism. Based on the binding score of -7.5 kcal/mol is shown in Table 2. The computational investigation concluded that compound T3 exhibited better binding energy than other analogs. The 3D docking images interaction for compound T3 with 4EY6 protein was shown in Figure 3.

Hydrogen bonding with MET 86 also interacts interact through lone pairs (S and N atoms) with surrounding amino acids. It Stabilizes ligands via polar interaction. Piperidine or alkyl chains in the ligand make van der Waals contact with ALA 753, stabilizing it in the lipophilic channel of AChE. Phenyl or aromatic substituents on ligands make π-π stacking or aromatic interaction with TYR 337. It Enhances ligand stacking and orientation. Thiadiazole aromatic extensions made with π-π stacking with TRP 86. It is common in AChE inhibitors for stacking with aromatic residues.

Table 2: Docking score of the synthesized compounds

S.No.	Synthesized compounds	Docking score
1	T 1	– 6.8
2	T 2	– 7.1
3	T 3	– 7.5
4	T 4	– 7.3
5	T 5	– 7.4

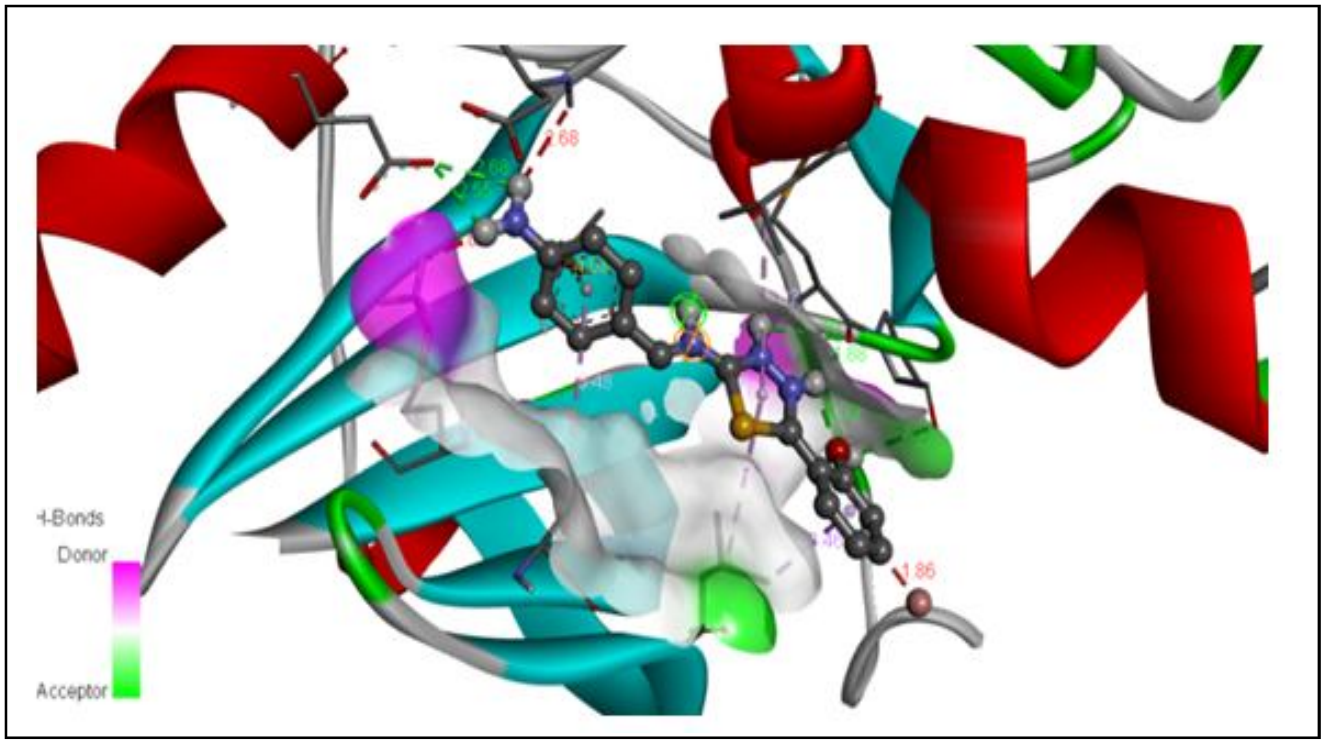

Figure 2: 3D docking interaction of compound T3 with 4EY6 protein.

Table 3: Effect of compound thiadiazole derivatives on cell viability in cultured SHSY5Y cells

Synthesized compounds	Test concentration (µg/ml) percentage viability					IC_{50} value(µg/ml)
	5	10	20	40	80	
T 1	98.62	86.09	64.80	37.19	22.57	43.21
T 2	99.48	94.97	67.20	65.49	77.83	43.95
T 3	97.77	88.77	71.75	30.12	21.24	42.43
T 4	98.11	91.28	69.93	36.63	21.77	44.11
T 5	96.56	86.26	68.42	33.80	20.58	127.87

3.3 *In vitro* evaluation

3.3.1 Effect of synthesized compounds on cytotoxicity induced by Aβ25-35 in SHSY5Y cells

Aβ25-35 (5-80 mol/l) treatment to SH-SY5Y cells for 48 h led to a dose-dependently substantially reduced cell viability in the medium. This study used a 25 µmol/l concentration of Aβ25-35 to examine how synthetic thiadiazole derivatives protected SH-SY5Y cells from neurotoxicity. In our initial step of studying the effects of synthetic compounds on Aβ25-35 neurotoxicities, we tested the viability of SH-SY5Y cells at various doses of the compounds (5, 10, 20, 40, and 80 µg/ml) to determine a non-cytotoxic concentration of the compounds. The SH-SY5Y cells were considerably protected from the cytotoxicity caused by Aβ25-35 when they were pretreated with 5-80 µg/ml of synthetic compounds for 30 min, which increased cell viability (Table 3). The cytotoxicity images are shown in Figure 4.

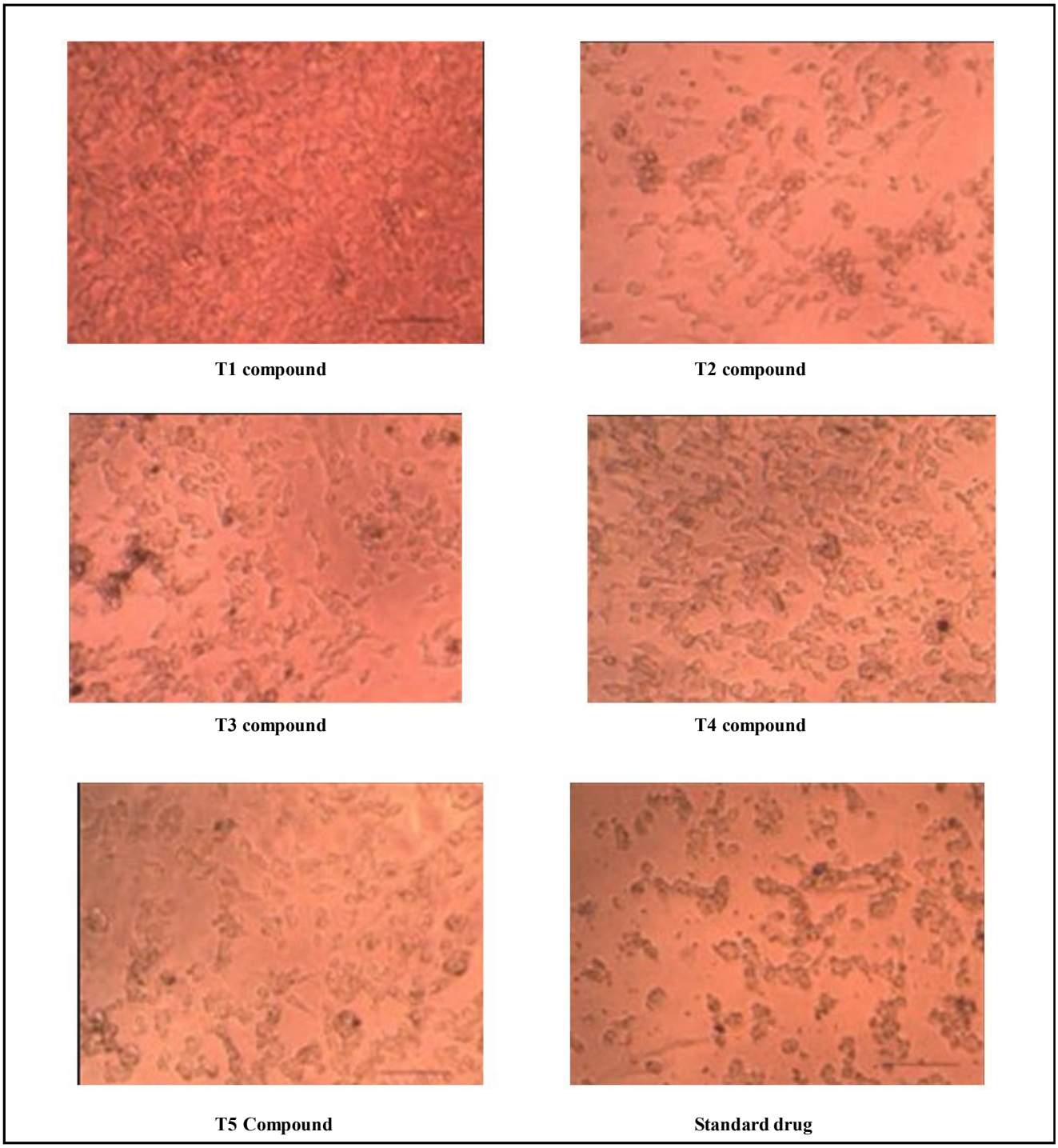

Figure 4: Cytotoxicity images for thiadiazole derivatives and standard drug.

T3 compound image showed densely populated, healthy-looking neuronal cells. Most cells are adherent, spread out, and exhibit a normal morphology. Mitochondrial activity was intact and supports mitochondrial stability, which reduces formazan crystals in the MTT assay. Since it measures mitochondrial dehydrogenase activity. The cell viability was high indicating low cytotoxicity. It maintains the membrane integrity and mitochondrial function and Inhibition of AChE (from the docking data). The bromophenol and –NH, substituent group in the T3 compound enhance hydrophilic-lipophilic balance, better membrane permeability, and reduced off-target toxicity. T3 compound has stronger and more stable binding to acetylcholinesterase (AChE), from docking results. Therefore, inhibiting AChE increases acetylcholine levels which protects neurons from degeneration in Alzheimer's disease. Compared with standard drugs Cells are fewer, rounded, and less adherent. Hence it indicated a loss of viability, especially at higher concentrations or longer exposure times. Possible cytotoxic effects, even though the drug was effective in enzyme inhibition. Neurons are more sensitive to standard drug stress, possibly due to mitochondrial disruption or apoptosis.

4. Discussion

The 1,3,4-thiadiazole scaffold is a privileged structure in medicinal chemistry, widely explored for neurological diseases due to its electron-rich, planar structure that facilitates π-π stacking with aromatic residues in enzymes like AChE, Capacity to form multiple hydrogen bonds due to its sulfur and nitrogen atoms, Potential for lipophilic interactions when substituted with hydrophobic groups like halogens or aromatic moieties. Synthesized thiadiazole derivatives (T1-T5) among these compound T3 ((E)-2-(5-((4-amino benzylidene)amino)-1,3,4-thiadiazol-2-yl)-5-bromophenol), smartly integrates this scaffold with pharmacophoric features, a phenolic OH group for hydrogen bonding, para-amino substituted aromatic ring that increases aqueous solubility and provides sites for interaction with acidic residues. The stepwise synthesis involved, the formation of the thiadiazole ring *via* cyclization of thiosemicarbazide and 4-bromo-salicylic acid, creating a reactive amine-substituted core. Subsequent schiff base formation with various aldehydes, especially para-aminobenzaldehyde for T3, leads to imine linkage (–CH=N–) with tunable electronic properties (Singh *et al*., 2022).

The docking studies revealed that T3 formed stable and significant interactions at the catalytic active site (CAS) and peripheral anionic site (PAS) of AChE. So, hydrogen bonds with MET 86 and SER 122 (docking image), π-π stacking with TRP 86 or TYR 337, critical for cholinesterase activity, the para-amino group enhanced hydrogen bonding and electrostatic interactions and the bromine atom facilitated halogen bonding and increased membrane permeability due to its lipophilic nature. The superior docking score of T3 compared to its analogs supports its potential as a dual-binding site AChE inhibitor, blocking both catalytic hydrolysis and amyloid-β aggregation (Zhao *et al*., 2021).

The MTT cytotoxicity assay clearly showed higher cell viability in T3-treated groups compared to standard drugs and other derivatives, minimal morphological damage (less cell shrinkage or apoptosis), and likely protection of mitochondrial integrity, indicating anti-apoptotic properties. This suggests that T3 not only inhibits AChE but also potentially reduces oxidative stress and cellular toxicity, both of which are central to AD pathology.

The neuroprotective effect of T3 may result from multi-target actions, such as AChE inhibition (improves cognitive function), prevention of amyloid β aggregation via binding at the PAS of AChE, and potential modulation of inflammatory markers. This aligns with the modern multi-target directed ligand (MTDL) strategy in AD drug design, as no single mechanism alone can effectively halt neurodegeneration.

This study introduces a novel series of 1,3,4-thiadiazole-based Schiff base derivatives incorporating a 5-bromophenol scaffold, designed for acetylcholinesterase (AChE) inhibition and neuroprotective activity relevant to Alzheimer's disease. The synthesized compounds (T1-T5), among these (T3) (E)-2-(5-((4-aminobenzylidene) amino)-1,3,4-thiadiazol-2-yl)-5-bromophenol exhibited the most promising results, displaying superior docking affinity toward the AChE active site (PDB: 4EY6) *via* key interactions such as hydrogen bonding and π-π stacking. The compound design is structurally novel, combining electron-donating and hydrophilic substituents (*e.g*., –OH, –NH, $–OCH_2$) that not only enhance receptor binding but also reduce lipophilicity-related toxicity.

To further ensure safety, synthetic steps were optimized using green chemistry approaches, such as the use of mild solvents and conditions, and avoiding toxic or heavy-metal catalysts. The *in vitro* MTT assay on neuronal cell lines revealed low cytotoxicity and high viability, affirming the compound's neuroprotective potential over standard AChE inhibitors. Additionally, the structure was thoroughly characterized using IR, NMR, and mass spectroscopy, while molecular docking and ADMET predictions supported its drug-likeness and safety profile. This integrative design combining rational drug design, synthetic innovation, and biological validation is marked as a significant advancement in the search for safer and effective therapeutic candidates for neurodegenerative disorders.

Additionally, the synthesis of 1,3,4-thiadiazole-based derivatives to reduce toxicity while preserving potent neuroprotective activity. Traditional AChE inhibitors such as tacrine and donepezil, though effective, are often limited by dose-dependent hepatotoxicity and gastrointestinal side effects (Kumar *et al.,* 2023). To address these concerns, the present work employs phenolic and Schiff base modifications of the thiadiazole core, which are known to enhance target specificity and antioxidant potential, thereby minimizing off-target interactions and cellular toxicity (Aliabadi *et al.,* 2024). *In vitro* MTT assays demonstrated that the synthesized derivatives, particularly the T3 compound, showed lower cytotoxicity and higher cell viability compared to the standard drug, indicating a favorable safety profile. Furthermore, molecular docking results confirmed selective and stable interactions with the active site of acetylcholinesterase (PDB: 4EY6) without disrupting key physiological residues, suggesting enhanced therapeutic potential with reduced side effects (Mehta *et al.,* 2022). Thus, this study introduces a novel scaffold with improved biocompatibility, representing a safer alternative in the development of anti-Alzheimer agents.

5. Conclusion

The design, synthesis, molecular docking, and biological assessment of novel (*E*)-2-(5-((arylidene) amino)-1,3,4-thiadiazol-2-yl)-5-bromophenol derivatives are emerging as highly potential therapeutic agents due to their ability to effectively target specific biological

pathways and exhibit diverse pharmacological activities options for AD are successfully demonstrated in this study. Docking's study demonstrated that T3 exhibited good interactions at the target protein's active site (PDB: 4EY6) and a considerable acetylcholinesterase (AChE) binding affinity among the synthesized compounds. In MTT assays, the compounds also showed improved neuroprotective potential with reduced cytotoxicity in comparison to conventional medications, suggesting a safer therapeutic profile. The thiadiazole ring's phenolic and Schiff base groups, among other structural elements, enhanced its effectiveness and decreased its toxicity. These results demonstrate how promising these thiadiazole derivatives are as lead molecules for more preclinical research in the treatment of Alzheimer's disease.

Acknowledgments

The author thanks the management and staff, Department of Pharmaceutical Chemistry and Analysis, School of Pharmaceutical Sciences, Vels Institute of Science, Technology and Advanced Studies (VISTAS), and the company for lending us the raw materials and workspace necessary to complete this work.

Conflicts of interest

The authors declare no conflicts of interest relevant to this article.

References

Afroz Patan and M. Vijey Aanandhi (2023). Thiazole chalcones: Promising agents with diverse pharmacological properties. Ann. Phytomed., **12**(1):230-240.

Ahmad Mohammadi Faran; Milad Takes; Mahsa Mohammadi; Amin Hosseini; Amin Aliabadi and Alireza Aliabadi. (2024). Synthesis, docking, and acetylcholinesterase inhibitory evaluation of 1,3,4-thiadiazole derivatives as potential anti-Alzheimer agents. Pharma. Sci., **30**(3): 369-378.

Ahmed, S.; Khan, M.; Ali, R.; Hussain, A.; Rehman, S. and Malik, A. (2020). Synthesis and evaluation of antimicrobial activity of 1,3,4-thiadiazole derivatives. Chem. Select., **5**(12):3678-3685.

Aliabadi, A.; Rezaei, Z.; Mahdavi, M.; Mohammadi, M.; Tavakkoli, M. and Shafiee, A. (2024). Synthesis and biological evaluation of 1,3,4-thiadiazole derivatives with reduced toxicity profiles. Pharma. Chem. J., **57**(2):118-121.

Altintop, M.D.; Sever, B.; Kaplancikli, Z.A.; Ali, T.; Koga, R. and Fujita, M. (2018). Design, synthesis, and biological evaluation of novel 1,3,4-thiadiazole derivatives as potential antitumor 55 agents against chronic myelogenous leukemia: Striking effect of nitrothiazole moiety. Molecules, **23**(1):59.

Anthwal, T.; Singh, H. and Nain, S. (2022). 1,3,4 Thiadiazole Scaffold: Antimicrobial Agents. Pharm. Chem. J., **12**:1345-1358.

Chandra Sekhar, D.; Rao, V.S.; Reddy, V.S.; Suresh, G.; Kumar, K.P. and Srinivas, M. (2019). Design and synthesis of 1,3,4-thiadiazole derivatives as novel anticancer and antitubercular agents. Russian J. General Chem., **89**:770-779.

Chen, L.; Zhang, Y.; Wang, Y.; Li, X.; Zhao, H. and Liu, Q. (2022). Synthesis, docking, and biological evaluation of thiadiazole and oxadiazole derivatives. J. Mol. Structure, **1256**:132594.

Elkina, N.A.; Makhaeva, G.F.; Rudakova, E.V.; Boltneva, N.P.; Lushchekina, S.V. and Bachurin, S.O. (2022). New multifunctional agents for potential Alzheimer's disease treatment based on tacrine conjugates. Biomolecules, **12**(11):1551.

Gowda, K.; Swarup, H.A.; Nagarakere, S.C.; Rangappa, S.; Kanchugarkoppal, R.S. and Kempegowda, M. (2020). Structural studies of 2,5-disubstituted 1,3,4-thiadiazole derivatives from thioesters under the mild condition: Studies on antioxidant, antimicrobial activities, and molecular docking. Synthetic Communications, **50**(10):1528-1544.

Halit Muðlu; Mustafa Akýn, M.; Serdar Çavuþ; Hasan Yakan; Neslihan Þaki and Emre Güzel. (2022). Exploring of antioxidant and antibacterial properties of novel 1,3,4-thiadiazole derivatives: Facile synthesis, structural elucidation, and DFT approach to antioxidant characteristics. Computational Biol. Chem., **96**:107618

Hatami, M.; Basri, Z.; Sakhvidi, B.K. and Mortazavi, M. (2023). Thiadiazole - A promising structure in the design and development of anti-Alzheimer agents. Int. Immunopharmacol., **118**:110027.

Kumar, R.; Mehta, M.; Sharma, A.; Arora, S.; Ali, F. and Singh, B. (2023). Design and development of safer AChE inhibitors: A structure-based approach. European. J. Med. Chem., **258**:115595.

Kumar, V.; Sharma, R.; Singh, A.; Gupta, N.; Mehta, K. and Verma, S. (2023). Synthesis and biological evaluation of new 1,3,4-thiadiazole derivatives. J. Hetero. Chem., **60**(3):456-462.

Kumar, A.; Singh, R.; Sharma, V.; Gupta, R.; Verma, R. and Mehta, M. (2022). Synthesis and characterization of new 1,3,4-thiadiazole derivatives. RSC Advances., **12**(24):14567-14575.

Li, J.; Sun, H.; Wang, Y.; Zhang, L.; Liu, X. and Yang, Z. (2021). Design, synthesis, and biological evaluation of 1,3,4-thiadiazole derivatives as potential anticancer agents. Bioorg. Med. Chem. Letters, **31**(2):127-133.

Mehta, M.; Sharma, A.; Kumar, R.; Ahmed, S.; Javed, H. and Singh, B. (2022). Current status and future perspectives of acetylcholinesterase inhibitors for Alzheimer's disease. Frontiers. Aging. Neurosci., **14**:874291.

Makhaeva, G.F.; Kovaleva, N.V.; Rudakova, E.V.; Boltneva, N.P.; Grishchenko, M.V.; Lushchekina, S.V.; Astakhova, T.Y.; Serebryakova, O.G.; Timokhina, E.N.; Zhilina, E.F.; Shchegolkov, E.V.; Ulitko. M.V.; Radchenko, E.V.; Palyulin. V.A.; Burgart, Y.V.; Saloutin, V.I.; Bachurin, S.O. and Richardson, R.J. (2023). Conjugates of tacrine and salicylic acid derivatives as new promising multitarget agents for Alzheimer's disease. Int. J. Mol. Sci., **24**(3):2285-2320.

Makhaeva, G.F.; Lushchekina, S.V.; Boltneva, N.P.; Rudakova, E.V.; Kovaleva, N.V. and Bachurin, S.O. (2020). Conjugates of tacrine and 1,2,4-thiadiazole derivatives as new potential multifunctional agents for alzheimers disease treatment. Bio-organic Chem., **96**:103563.

Malarkodi Velraj, Afroz Patan, P. Shanmugasundaram, S. Jayakumari, A.Vijayalakshmi and Shyam Sundar (2024). Molecular docking studies of some natural phytochemical constituents as acetylcholinesterase and butyrylcholinesterase inhibitors. Ann. Phytomed., **13**(1):1046-1053.

Patel, M.N.; Patel, R.H.; Patel, S.R.; Shah, V.R.; Desai, K.R. and Patel, D.H. (2020). Synthesis and evaluation of antimicrobial activity of 1,3,4-thiadiazole derivatives. J.Chem. Sci., **132**(1):1-10.

Patel, D.; Shah, A.; Mehta, R.; Desai, S.; Joshi, H. and Patel, K. (2021). Design, synthesis, and biological evaluation of 1,3,4-thiadiazole derivatives as potential anticancer agents. Med. Chem., **17**(9):789-798.

Pham, E.C.; Nguyen, V.T.; Le, H.Q.; Tran, T.N.; Bui, Q.M. and Vo, D.V.N. (2022). Synthesis of novel 2-amino-5-substituted 1,3,4-oxadiazole and 1,3,4-thiadiazole derivatives. Med Chem., **18**(5):558-573.

Sindhu, T. J.; Jainey P. James; C. Zakiya Fathima; Merly Susan Babu and Akito Sheqi (2024). Molecular docking and pharmacophore modelling of Schiff base derived thiazolidinones as peroxiredoxin and tyrosinase inhibitors for oxidative stress. Ann. Phytomed., **13**(2):653-661.

Singh, R.; Kaur, P.; Sharma, S.; Gupta, A.; Mehta, M. and Arora, R. (2022). Synthesis, docking, and biological evaluation of thiadiazole and oxadiazole derivatives. Bioorg. Chem., **115**:105232.

Singh, P.; Kaur, R.; Sharma, N.; Gupta, M.; Arora, R. and Singh, S. (2021). Synthesis and biological evaluation of new 1,3,4-thiadiazole derivatives. Med. Chem. Res., **30**(5):789-798.

Shaikh, S.A.; Wakchaure, S.N.; Labhade, S.R.; Kale, R.R.; Alavala, R.R. and Chobe, S.S. (2024). Synthesis, biological evaluation, and molecular docking of novel 1,3,4-substituted-thiadiazole derivatives as potential anticancer agents. BMC Chemistry., **18**:119.

Zahid Ali; Wajid Rehman; Liaqat Rasheed; Abdullah Y; Alzahrani; Nawab Ali; Rafaqat Hussain, Abdul-Hamid Emwas; Mariusz Jaremko and Magda H. Abdellattif. (2023). New 1,3,4-thiadiazole derivatives as α-glucosidase inhibitors: Design, synthesis, DFT, ADME, and *in vitro* enzymatic studies. ACS. Omega. **8**(3):5854-5862

Zhou, Y.; Wang, X.; Li, H.; Liu, Z.; Chen, Y. and Zhang, J. (2023). Design, synthesis, and biological evaluation of 1,3,4-thiadiazole derivatives as potential anticancer agents. European J. Med. Chem., **245**:114789.

Zhao, X.; Li, Y.; Wang, J.; Chen, Z.; Liu, H. and Zhang, Q. (2021). Synthesis and evaluation of antimicrobial activity of 1,3,4-thiadiazole derivatives. J. Enzyme. Inhib. Med. Chem., **36**(1):123-130.

Zhang, Y.; Li, X.; Wang, Z.; Chen, H.; Liu, Y. and Zhao, J. (2022). Synthesis and evaluation of antimicrobial activity of 1,3,4-thiadiazole derivatives. Let. Drug Des. Dis., **19**(7):567-574.

Citation **E. Joel Mart and C. Ronald Darwin (2025). Novel thiadiazole derivatives targeting acetylcholinesterase in alzheimer's disease: Synthesis and biological evaluation. Ann. Phytomed., 14(1):559-568. http://dx.doi.org/10.54085/ap.2025.14.1.53.**